POLITECNICO DI TORINO
Repository ISTITUZIONALE

Advances in molecular quantum computing: From technological modeling to circuit design

Original
Advances in molecular quantum computing: From technological modeling to circuit design / Cirillo, G.A., Turvani, G., Simoni, M., Graziano, M.. - ELETTRONICO. - 2020-:(2020), pp. 132-137. (19th IEEE Computer Society Annual Symposium on VLSI, ISVLSI 2020 Limassol (Cyprus) 2020) [10.1109/ISVLSI49217.2020.00033].

Availability:
This version is available at: 11583/2846258 since: 2020-09-21T13:15:32Z

Publisher:
IEEE Computer Society

Published
DOI:10.1109/ISVLSI49217.2020.00033

Terms of use:

This article is made available under terms and conditions as specified in the corresponding bibliographic description in the repository

Publisher copyright
IEEE postprint/Author's Accepted Manuscript

©2020 IEEE. Personal use of this material is permitted. Permission from IEEE must be obtained for all other uses, in any current or future media, including reprinting/republishing this material for advertising or promotional purposes, creating new collecting works, for resale or lists, or reuse of any copyrighted component of this work in other works.

(Article begins on next page)

13 June 2026

Advances in Molecular Quantum Computing: from Technological Modeling to Circuit Design

Giovanni Amedeo Cirillo*, *Student Member, IEEE*, Giovanna Turvani*,
Mario Simoni*, *Student Member, IEEE*, and Mariagrazia Graziano†, *Member, IEEE*
*Department of Electronics and Telecommunications, Politecnico di Torino, Turin 10129, Italy
†Department of Applied Science and Technology, Politecnico di Torino, Turin 10129, Italy
Corresponding Authors: giovanni_cirillo@polito.it, giovanna.turvani@polito.it

***Abstract*—Molecules are serious candidates for building hardware for quantum computers. They can encode quantum information onto electron or nuclear spins and some of them show important features as the scalability of the number of qubits and a universal set of quantum gates.**
In this paper we present our advances in the development of a classical simulation infrastructure for molecular Quantum Computing: starting from the definition of simplified models taking into account the main physical features of each analyzed molecule, quantum gates are defined over these models, thus permitting to take into account the real behavior of each technology during the simulation. An interface with a hardware-agnostic description language has been also developed.
The knowledge of the behavior of real systems permits to optimize the design of quantum circuits at both physical and compilation levels. Elementary quantum algorithms have been simulated on three different molecular technologies by changing the physical parameters of polarization and manipulation and quantum circuit design strategies. Results confirm the dependency of the fidelity of the results on both levels, thus proving that the choice of optimal operating points and circuit optimization techniques as virtual-Z gates are fundamental for ensuring the execution of quantum circuits with negligible errors.

***Index Terms*—Molecular quantum computing, molecular nanomagnets, quantum computing architectures, innovative technology.**

I. Introduction

Spin has been always identified as a proper quantum system for encoding the quantum unit of information: its possible orientations can properly encode different qubit values and magnetic resonance techniques can be employed for implementing quantum gates [1]. An important family of spin qubits is the molecular one, where information is encoded onto nuclear or electron spins belonging to molecules. **Liquid-state NMR molecules** [2] - where spectroscopy apparatus is exploited for manipulating nuclear spins (usually H, C and F) - constitute the first technology on which quantum algorithms were experimentally executed [3] and they are still employed for testing quantum circuits [4], [5]. Unfortunately, the maximum number of qubits is limited to about ten because on the one hand the spin polarization at room temperature is poor, on the other spins chemical shifts - which are fundamental for ensuring the addressability of single qubits - may overlap.
The possibility of having natural quantum systems for qubit encoding makes molecular Quantum Computing still interesting and the synthesis of complex molecules with more spin qubits is required for overcoming the limitations of the traditional technology. Spin-switch-based technologies - in particular the supramolecular complexes based on **Cr_7Ni molecular nanomagnets** [6], [7] and a nuclear spin qubit architecture consisting of two weakly interacting **vanadyl moieties** [8] - result extremely interesting not only for their long relaxation and decoherence timescales and for their intrinsic easy implementability of an universal set of quantum gates, but also for their qubits scalability through supramolecular chemistry techniques, in particular the first one.
Since a definitive leader technology for quantum computation is not already established, it is important to understand which are the expected results of a designed quantum circuit on real quantum hardware; this can be achieved through a *via*-cloud access to quantum computers or simulating them on classical computers. An infrastructure for simulating molecular technologies for quantum computing on a classical computer, starting from what introduced in [9] for Cr_7Ni supramolecular complexes, has been developed in MATLAB environment and is here introduced: each molecule is described by a simplified physical model which must be sufficiently complete for ensuring a good mimic of the real quantum system and must require the minimum amount of computational resources. A model for the vanadyl architecture - also characterized by the spin switch mechanism - has been defined, together with a preliminary one for liquid-state NMR, tested on the heteronucleus ^{13}C-labeled diethyl fluoromalonate [5]. Even though its use is gradually reducing, NMR experimental results in the last twenty years permit to have a high amount of data for validating the simulator through comparison. Another important improvement with the respect to [9] is the insertion of non-ideality phenomena as relaxation and decoherence in the simulation mechanism.
Figure 1 shows the block scheme of the developed infrastructure: starting from a common simulation layer - evaluating the evolution of each quantum state due to electro-magnetic fields for the implementation of gates, relaxation and decoherence - a specific model of each technology is developed and interfaced with the lower level, taking into account the main and eventually exclusive features of each system and their dependencies on external parameters as magnetostatic fields and temperature. In order to simplify the quantum circuit design to users, the current infrastructure can be programmed in the

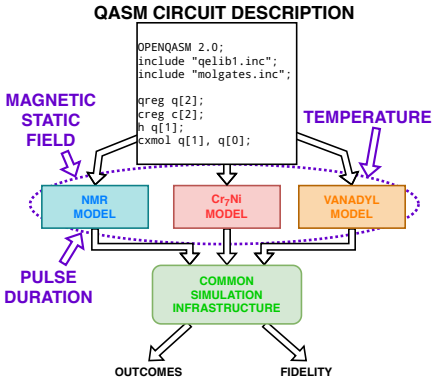

Fig. 1. Block scheme of the developed infrastructure.

quantum Hardware Description Language called **OpenQASM** [10], whose syntax is automatically translated into simulator routines. In any case, programming based on internal routines is available, in order to investigate alternative qubit's control strategies. The current simulation results are the expected real hardware outcomes and the fidelity [1].

After an overview of the main features of the analyzed molecular technologies, the current methodology for modeling the effects of non-ideality phenomena is described in Section III, then Section IV highlights the virtual-Z approach [11] for reducing the circuit latency. The developed simulator has been tested with different quantum circuits for each molecule and the main results are reported in Section V, where it is possible to ascertain that the choice of appropriate physical parameters and circuit optimization strategies can increase the fidelity of the outcomes of a quantum computer. Future perspectives for improving the infrastructure are reported in Section VI.

II. Modeling Molecular Technologies for Quantum Computing

Table I compares these technologies in terms of spin types, qubits connectivity, gates bandwith and coherence timescales. They can all implement an universal set of quantum gates consisting of single-qubit gates $R_{\{x,y,z\}}(\theta)$ and Controlled-Z (CZ) [1], [9]. The spin Hamiltonians of these molecular

TABLE I
Comparison of the molecular technologies currently available in the simulation infrastructure.

	NMR	Cr_7Ni rings	Vanadyl
Spin types	Nuclear	Electron	Nuclear (qubit) Electron (switch)
Qubits connectivity	Full	Linear	Linear
Quantum gates frequencies	RF ($R_k(\theta)$) Low Freq (CZ)	MW	RF ($R_k(\theta)$) MW (CZ)
Coherence timescales	1 s	600 ns (qubit) 2 µs (switch)	$\gg$ 1 µs (qubit) 1 µs (switch)

RF = Radio Frequency, MW = Microwave

systems, assuming a magnetic static field $\mathbf{B}_0 = B_0\mathbf{z}$ applied along the z-axis are reported in the following; it can be ascertained that they are all characterized by a term related to

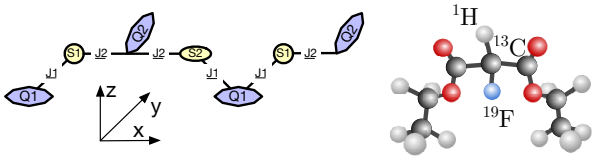

(a) Conceptual scheme of a four-qubit Cr_7Ni complex, where **Q** and **S** refer to a spin qubit and a spin switch respectively.

(b) ^{13}C-labeled diethyl fluoromalonate for NMR quantum computing with three qubits.

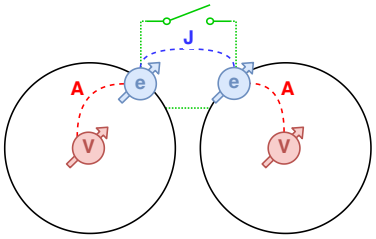

(c) Conceptual scheme of the vanadyl architecture.

Fig. 2. Modeled molecules in the current version of the simulator infrastructure.

single-qubit gates and another one related to two-qubit gates and the Pauli matrix $\sigma_z = \mathrm{diag}([+1, -1])$ is always present. The simplest form of the Hamiltonian for a system of coupled nuclear spins is

$$\frac{\mathcal{H}_{\mathrm{NMR}}}{\hbar} = -\frac{1}{2}\sum_i \omega_{0_i}\sigma_{z_i} + \frac{1}{4}\sum_{i<j} 2\pi J_{ij}\sigma_{z_i}\sigma_{z_j}, \qquad (1)$$

where ω_{0_i} is the transition frequency of the i^{th} spin-$\frac{1}{2}$ and J_{ij} is the through-bond coupling strength of i^{th} and j^{th} spins, depending on the respective nuclear species and decreasing with the number of chemical bonds separating the nuclei. The first term of the Hamiltonian involves each spin independently from the others and is related to the implementation of single-qubit gates, while the second one involves pairs of spins and is exploited for implementing two-qubit gates. NMR quantum computers usually show $\max\{2\pi J_{ij}\} \ll \min\{\Delta\omega_0\}$, where $\min\{\Delta\omega_0\}$ is the minimum difference between single-qubit transition frequencies, thus single-qubit gates can be applied on each spin with negligible effects of spin-spin interactions for timescales $\tau \ll \frac{1}{\max(J_{i,j})}$.

The Hamiltonian of Cr_7Ni supramolecular complexes is

$$\begin{aligned}\frac{\mathcal{H}_{\mathrm{CrNi}}}{\hbar} =& \mu_{\mathrm{B}}\frac{1}{2}\sum_{i=1}^{N}\left(g_{z_{i_{\mathrm{qubit}}}}B_0\sigma_{z_{i_{\mathrm{qubit}}}}\right) + \mu_{\mathrm{B}}\frac{1}{2}\sum_{i=1}^{N-1}\left(g_{z_{i_{\mathrm{sw}}}}B_0\sigma_{z_{i_{\mathrm{sw}}}}\right)\\ &+ \frac{1}{4}\sum_{i=1}^{N-1}\left(J_{z_{i_{\mathrm{qubit}},i_{\mathrm{sw}}}}\sigma_{z_{i_{\mathrm{qubit}}}}\sigma_{z_{i_{\mathrm{sw}}}}\right)\\ &+ \frac{1}{4}\cdot\sum_{i=1}^{N-1}\left(J_{z_{i_{\mathrm{sw}},i+1_{\mathrm{qubit}}}}\sigma_{z_{i_{\mathrm{sw}}}}\sigma_{z_{i+1_{\mathrm{qubit}}}}\right),\end{aligned} \qquad (2)$$

where μ_B is the Bohr's magneton, J_z is the z-axis term of the anisotropic exchange tensor describing the interaction between

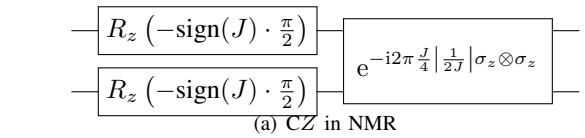

(a) CZ in NMR

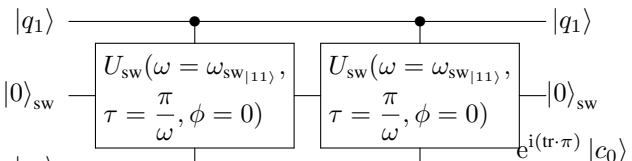

(b) CZ in Cr_7Ni rings and vanadyl. In the accumulated phase $\mathrm{e}^{\mathrm{i}(\text{tr}\cdot\pi)}$, tr $= 1$ when two resonant transitions were done on the switch and 0 otherwise.

Fig. 3. CZ gate implementations with analyzed molecular technologies

adjacent spins and g_z is the z-axis term of the spectroscopic tensor describing the interaction of the magnetic moments with an external magnetic field. Considering Figure 2(a), the molecule is characterized a periodical structure, where J_z and g_z assume only two values in a regular way. Magnetic anisotropy is responsible for different transition frequencies of spin qubits - thus allowing their independent rotation - and for a transition frequency shift of the spin switch depending on the states of the adjacent spin qubits, exploited for implementing the CZ gate. The parameters of the molecule employed in simulations are available in [6] and [7].

The vanadyl architecture is based on two vanadium ions with both electronic and nuclear spins (spin-$\frac{7}{2}$) not directly connected by a bridging ligand, so the most relevant magnetic interaction is expected to be the dipolar through-space one [8]. The system is described by the following Hamiltonian

$$\frac{\mathcal{H}_{\text{vanadyl}}}{\hbar}=\sum_{i=1}^{2} I_{z_i}A_{z_i}\sigma_{z_i}+\mu_B\frac{1}{2}\sum_{i=1} g_{z_i}B_0\sigma_{z_i}+\frac{J}{2}\sigma_{z_1}\sigma_{z_2}, \tag{3}$$

where $I_z = \text{diag}\left(\left[+\frac{7}{2},+\frac{5}{2},\cdots,-\frac{5}{2},-\frac{7}{2}\right]\right)$, J describes the interaction between electronic spins while A is the hyperfine interaction between nuclear and electronic spins. For $B > 0.3\,\text{T}$ spin states are practically factorized because of the large difference in their Zeeman energies - so the rotation of each nuclear spin does not depend on the state of the other - while the rotation of coupled electron spins depends on the state of both nuclei, because of the hyperfine coupling. Therefore the eigenstates $\left|+\frac{7}{2}\right\rangle$ and $\left|+\frac{5}{2}\right\rangle$ of nuclear spins encode qubits while the electron ones are exploited for encoding the switch for the CZ gate.

An important consequence of the different mechanisms for implementing the two-qubit gate (J-coupling in NMR, rotation frequency shift of the intermediate spin switch in the other molecules, see Figure 3) is that the timescales of two-qubit gates can strongly affect the fidelity of the results. In fact, while the frequency shift of the spin switch rotation frequency does not require to change the gate duration, the CZ duration in NMR is in the order of $\tau = \left|\frac{1}{2J}\right|$ (see Figure 3(a)), which is not certainly much lower than the timescales of non-idealities as relaxation and decoherence. Moreover, in a system with multiple spin qubits, it cannot be ensured that in the same time interval other qubit-qubit interactions provide a negligible contribution, so refocusing techniques [1] for compensating these must be applied on the qubits not involved in the gate of interest.

III. Development of noisy simulations

The model proposed in [9] has been improved by introducing the density matrix formalism for including the effects of non-idealities in simulation.

The mixed state of an open quantum system interacting with an external environment can be described by a density matrix

$$\rho=\sum_i p_i\left|\psi_i\right\rangle\left\langle\psi_i\right|, \tag{4}$$

where p_i is a classical probability and $|\psi_i\rangle$ is the state vector of a pure state as $|0\rangle$ or $\frac{|0\rangle+|1\rangle}{\sqrt{2}}$, whose density matrix would be simply $\rho = |\psi\rangle\langle\psi|$. The density matrix of a n-qubit system is complex and square of order 2^n and its main diagonal corresponds to the probability distribution of the basis states $|0\cdots0\rangle, \cdots, |1\cdots1\rangle$, thus $\sum_{i=0}^{2^n-1}\rho_{i,i}=1$. While the unitary evolution $U(t)$ associated to a quantum gate changes a state vector according to $|\psi_U\rangle = U(t)\cdot|\psi\rangle$, a density matrix evolves according to

$$\rho_U = U(t)\cdot\rho\cdot U^\dagger(t) \tag{5}$$

With this formalism, it is possible to model the main non-ideality phenomena of the analyzed technologies:

- **relaxation**, which is the loss of energy of an excited quantum state;
- **decoherence**, related to the qubit's phase loss;
- **residual qubit-qubit interaction**, which does not insulate qubits and is described by a unitary matrix.

Relaxation and decoherence are described by non-unitary matrices whose models are proposed in Section III-B.

A. Simulation strategy

The effects of non-idealities are evaluated in terms of fidelity [1], given by

$$\mathcal{F}=\sqrt{\langle\psi_{\text{ideal}}|\,\rho\,|\psi_{\text{ideal}}\rangle}\in\mathbb{R}, \tag{6}$$

where $|\psi_{\text{ideal}}\rangle$ is the state vector of the ideal state in which the quantum system would be after applying the gates of the simulated quantum circuit. It is possible to prove that $0 \leq \mathcal{F} \leq 1$.

In order to evaluate the effects of these phenomena during a simulation, it is assumed that:

- the system is initialized in its ground state, corresponding to a density matrix $\rho_{\text{init}} = |0\cdots0\rangle\langle0\cdots0|$;
- each quantum gate is applied for a time amount τ, thus changing ρ and $|\psi_{\text{ideal}}\rangle$, and in the same time interval the effects of non idealities on the density matrix are estimated;
- after a measurement operation call, the probability distribution of the quantum system - corresponding to the main diagonal of ρ - is provided.

This simulation procedure was thought for Cr_7Ni molecular nanomagnets and then extended to vanadyl and liquid-state NMR technologies, with some aware limitations as the spin-$\frac{1}{2}$ manipulation model for the first technology (qubits are encoded onto spin-$\frac{7}{2}$, but the transition $\Delta E_{|+\frac{5}{2}\rangle \to |+\frac{3}{2}\rangle} \gg \Delta E_{|+\frac{7}{2}\rangle \to |+\frac{5}{2}\rangle}$) and the initial fiducial state $|0\cdots 0\rangle\langle 0\cdots 0|$ for the second one (it is a thermal mixture from which a pseudo-pure initial state can be derived).
Even though computation and manipulation of matrices are heavy from a computational point of view, it is important to precise that the use of an optimized software for linear algebra numerical calculations like MATLAB and low number of qubits of the analyzed molecules ensure the simulation of quantum algorithms on classical machines in execution times of at most some second.

B. Models for relaxation and decoherence

Relaxation and decoherence are described by non-unitary matrices which affect the density matrix according to an element-by-element matrix multiplication (.* in MATLAB), in order to have a computationally easy mimic of the single-qubit density matrix evolution due to these phenomena [1]:

$$\begin{bmatrix} (a-a_0)\mathrm{e}^{-\frac{t}{T_1}}+a_0 & b\mathrm{e}^{-\frac{t}{T_2}} \\ b^*\mathrm{e}^{-\frac{t}{T_2}} & (a_0-a)\mathrm{e}^{-\frac{t}{T_1}}+1-a_0 \end{bmatrix} \tag{7}$$

Relaxation is modeled by a matrix

$$R = \bigotimes_{i=n-1}^{0} \begin{bmatrix} 1 & 1 \\ 1 & \mathrm{e}^{-\frac{t}{T_{1,i}}} \end{bmatrix}, \tag{8}$$

where $\bigotimes$ refers to a Kronecker product involving n qubits and $T_{1,i}$ is the relaxation time constant of the i^{th} qubit and t is the time duration in which relaxation is evaluated. The terms on the main diagonal of R, with the exception of that on the top left associated to the ground basis state $|0\cdots 0\rangle$, are always lower than 1, thus permitting to describe their loss of probability. In order to computationally simplify the description of relaxation, the probability loss is always provided to the ground state, according to the following procedure:

1) compute the element-by-element product $\rho_{\text{el-by-el}_{i,j}} = R_{i,j}\rho_{i,j}$;
2) compute the excited levels loss term as $l = \sum_{i=1}^{2^n-1}(1-R_{i,i})\rho_{i,i}$ and add it to $\rho_{\text{el-by-el}_{0,0}}$;
3) assign $\rho_{\text{el-by-el}}$ to ρ.

This procedure preserves $\sum_{i=0}^{2^n-1}\rho_{i,i} = 1$.
Decoherence is modelled by a matrix

$$D = \bigotimes_{i=n-1}^{0} \begin{bmatrix} 1 & \mathrm{e}^{-\frac{t}{T_{2,i}}} \\ \mathrm{e}^{-\frac{t}{T_{2,i}}} & 1 \end{bmatrix}, \tag{9}$$

where $T_{2,i}$ is the decoherence time constant of the i^{th} qubit. In this case the element-by-element product is sufficient.
The values of $T_{\{1,2\},i}$ are characteristic of the model of each technology and eventually computed according to a set of external variables as magnetostatic field and temperature. These are then provided to the common simulator infrastructure (see Figure 1) before launching the simulation. It is clear that longer is the execution time of a quantum circuit, more significant are the effects of relaxation and decoherence, so the definition of circuit compilation strategies for minimizing the number of effective gates to be applied on hardware are required for having higher fidelity on the results.

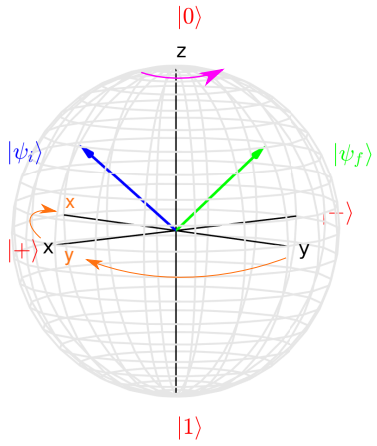

Fig. 4. Representation of Virtual-Z principle on the Bloch sphere. The final state $|\phi_f\rangle = R_z\left(\frac{\pi}{2}\right)|\psi_i\rangle$ can be achieved by rotating the z-axis by $\frac{\pi}{2}$ or rotating the x and y axes by $-\frac{\pi}{2}$.

IV. Spin-$\frac{1}{2}$ manipulation and virtual-Z gates

Operations on a qubit correspond to moving the state vector through rotations by an amount θ of the Cartesian axes described by matrices $R_x(\theta)$, $R_y(\theta)$, $R_z(\theta)$ [1]. It is possible to prove that any arbitrary single-qubit gate can be constructed as [10]

$$\begin{aligned} U_3(\theta,\phi,\lambda) &= \begin{bmatrix} \cos\left(\frac{\theta}{2}\right) & -\mathrm{i}\mathrm{e}^{\mathrm{i}\lambda}\sin\left(\frac{\theta}{2}\right) \\ -\mathrm{i}\mathrm{e}^{\mathrm{i}\phi}\sin\left(\frac{\theta}{2}\right) & \mathrm{e}^{\mathrm{i}(\lambda+\phi)}\cos\left(\frac{\theta}{2}\right) \end{bmatrix} = \\ &= R_z(\phi)R_x(\theta)R_z(\lambda) \\ &= R_z\left(\phi-\frac{\pi}{2}\right)R_x\left(\frac{\pi}{2}\right)R_z\left(\pi-\theta\right)R_x\left(\frac{\pi}{2}\right)R_z\left(\lambda-\frac{\pi}{2}\right) \end{aligned} \tag{10}$$

In the case of a spin-$\frac{1}{2}$ system, its two eigenstates $\left|\pm\frac{1}{2}\right\rangle$ show an energy difference $\Delta E = \hbar\omega_0$ when it is subjected to a magnetostatic field. If this is applied along the z-axis, the spin state is changed by an oscillating magnetic field on the xy-plane with frequency equal to ω_0 and on a time interval τ (sinusoidal field modulated by a port signal). The spin-$\frac{1}{2}$ unitary evolution in a frame rotating with frequency ω_0 around the z-axis can be written as

$$\begin{aligned} U &= \begin{bmatrix} \cos\left(\frac{\omega_1\tau}{2}\right) & \sin\left(\frac{\omega_1\tau}{2}\right)\mathrm{e}^{-\mathrm{i}\left(\frac{\pi}{2}+\phi\right)} \\ \sin\left(\frac{\omega_1\tau}{2}\right)\mathrm{e}^{-\mathrm{i}\left(\frac{\pi}{2}-\phi\right)} & \cos\left(\frac{\omega_1\tau}{2}\right) \end{bmatrix} \\ &= U_3(\omega_1\tau,\phi,-\phi), \end{aligned} \tag{11}$$

where ω_1 is proportional to the amplitude of the oscillating magnetic field. The amount of spin rotation is given by $\theta = \omega_1\tau$, while the rotation axis on the xy-plane depends on the initial oscillation phase ϕ, with $R_x(\theta)$ and $R_y(\theta)$ gates given by $\phi = 0$ and $\phi = \frac{\pi}{2}$ respectively.

With Equation 11, $R_z(\theta)$ can be implemented as $R_z(\theta) = HR_x(\theta)H$, where $H \simeq R_x(\pi)R_y\left(\frac{\pi}{2}\right)$ is the Hadarmard gate, so it requires five consecutive gates which would be preferably avoided. However, observing that the effect on the state vector of $R_z(\theta)$ is the same of rotating the x and y axes by $-\theta$ (see Figure 4), it is possible to keep the effect of $R_z(\theta)$ without applying any physical quantum gate [11] by changing the phases associated to $R_{x,y}(\theta)$ according to the following procedure:

$$x: \ \phi_x \rightarrow \phi_x - \theta \qquad y: \ \phi_y \rightarrow \frac{\pi}{2} + \phi_x - \theta \qquad (12)$$

where ϕ_x and ϕ_y are the phases of the external oscillations for implementing $R_x(\theta)$ and $R_y(\theta)$ respectively. The so-called **virtual-Z** approach implies that $R_z(\theta)$ gates are atomic, *i.e.* they do not require any loss of time. Considering Equation 10, at most one variable-amplitude-and-phase ($R_x(\theta)$) or two only-variable-phase ($R_x(\frac{\pi}{2})$) oscillations are required for implementing a single-qubit gate. For example, virtual-Z strategy ensures the implementation of Hadamard gate with only one pulse, since it can be also obtained as $R_z\left(\frac{\pi}{2}\right)R_x(\frac{\pi}{2})R_z\left(\frac{\pi}{2}\right)$. It is clear that maximizing R_z gates is a precious resource for reducing the number of pulses to be applied on qubits and then the effects of dynamical non-idealities.

V. Results

The interface with OpenQASM permits to design quantum circuits without a knowledge of all the routines of the MATLAB-based simulator and to evaluate the fidelity of their execution. The simulation results for four molecules (two and three-qubit Cr_7Ni supramolecular complexes, vanadyl architecture and the NMR heteronucleus ^{13}C-labeled diethyl fluoromalonate) are reported. It is assumed that pulse duration is fixed, while amplitude and phase of the oscillation of single-qubit gates can be freely changed, on the one hand for having continuity with the model described in [9], on the other because it is theoretically a simple use case of fidelity increase due to virtual-Z strategy. Moreover, refocusing is assumed to be always applied in NMR simulations for removing undesired interactions. The relaxation and decoherence timescales are either taken from previous works or estimated considering some experimental data or assumed in a bad-case scenario. The results are all provided in terms of fidelity $\mathcal{F}_{\text{virt}Z}$ and $\frac{\mathcal{F}_{\text{virt}Z}}{\mathcal{F}_{\text{Nvirt}Z}} - 1$, *i.e.* its relative enhancement exploiting virtual-Z approach instead of the typical one.

Figures 5 and 6 show the fidelity dependency on different physical parameters for Cr_7Ni and vanadyl architectures: as expected, fidelity gradually reduces when the duration of quantum gates increases and when the magnetostatic field reduces or temperature increases because of a reduction of T_2, while the reduction of single-qubit gates due to virtual-Z increases the fidelity with the same pulse duration (Figures 5(b) and 6(b)).

Tables II and III report $\mathcal{F}_{\text{virt}Z}$ and $\frac{\mathcal{F}_{\text{virt}Z}}{\mathcal{F}_{\text{Nvirt}Z}} - 1$ (in parentheses). The pulse durations were chosen coherently with the those indicated in the references. As in the plotted cases, a fidelity enhancement is always present, in particular for Cr_7Ni molecules, characterized by shorter non-idealities timescales than the others. In the vanadyl case, the fidelity values seem to be quite low, but it is important to precise that a quite bad scenario for $T_{\{1,2\}}$ was chosen. NMR shows fidelities all over 90%, with an interesting higher fidelity enhancement for Grover's algorithm, Quantum Fourier Transform and Quantum Phase Estimation due to a significant reduction of the number of pulses for Hadamard or Cϕ (with $\phi \neq \pi$) gates.

VI. Conclusions

An overview of the current advances in molecular quantum computing modeling and design has been presented. It has been ascertained that a complete simulation infrastructure depends on several variables and optimal design can be done on multiple levels: from physical parameters for polarization and manipulation to quantum circuits compilation strategies. Even though the model is still quite preliminary, it has already reached a sufficient maturity for establishing a future roadmap, assuming that the proposed model-based methodology can be optimistically extended to other molecular technologies for Quantum Computing.

From the simulation point of view, the computational and storage difficulties related to standard density matrix formalism of many-qubit systems should be overcome with alternative representations of noisy quantum states, analogous to what already done for state vectors [12]. Moreover, the investigation of other manipulation strategies as fixed-amplitude RF fields and variable pulse duration, models for manipulating spins $S > \frac{1}{2}$, the systematic insertion of the effects of gates error (*e.g.* due to a Gaussian signal modulation instead of a port one) and a measurement model are important for having a good mimic of these molecular technologies.

For what concerns the physical level, the experimental or simulated analysis of the dependency of parameters as T_1 and T_2 on the highest possible number of external variables is the first fundamental operation to be done for estimating accurate parameters to be provided to the simulator.

At circuit level, it has been proved that virtual-Z gates effectively increase the fidelity of quantum circuits, in particular for technologies where the non-ideality timescales are not much longer than those of quantum circuits, but they are not sufficient for maximizing the fidelities of the results. *Ad-hoc* circuit optimization strategies based on the native gates of these molecules must be defined in order to achieve this goal. NMR models are still quite preliminary and the first activities to be done in order to increase their reliability should be the initialization from a pseudo-pure state, the inclusion of models for homonuclear molecules and output measurement procedures as the quantum state tomography.

We hope that this system can be a starting point for having an accurate infrastructure for classical simulations of molecular quantum computers, which will ensure in future a hardware-reliable quantum circuit design. In order to achieve this goal the interaction between circuit designers and experimentalists - in terms of validation of simplified models and fruition of experimental results - is necessary.

TABLE II
FIDELITY EMPLOYING VIRTUAL-Z GATES FOR TWO-QUBIT CIRCUITS

Circuit	Cr_7Ni ($\tau = 25\,ns$, $B = 7\,T$, $T_{1,qubit} = 17\,\mu s$, $T_{2,qubit} = 680\,ns$, $T_{2,switch} = 2.3\,\mu s$)	Vanadyl ($\tau_s = 10\,\mu s$, $\tau_d = 150\,ns$, $T_{1,qubit} = 1.0\,s$, $T_{2,qubit} = 0.5\,s$, $T_{2,switch} = 0.5\,\mu s$)	NMR ($\tau = 25\,\mu s$, $T_{1,min} = 3.0\,\mu s$, $T_{2,min} = 1.2\,\mu s$)
bell	96.67% (+4.65%)	92.91% (+0.23%)	99.86% (+0.05%)
swap01	95.55% (+3.02%)	89.62% (+0.14%)	99.68% (+0.11%)
deujos_b	92.02% (+14.72%)	86.75% (+0.38%)	99.73% (+0.12%)
grover10	87.77% (+6.75%)	86.60% (+0.34%)	99.70% (+0.12%)
qft2	89.94% (+11.50%)	86.45% (+0.52%)	99.72% (+0.18%)

TABLE III
FIDELITY EMPLOYING VIRTUAL-Z GATES FOR THREE-QUBIT CIRCUITS

Circuit	Cr_7Ni ($\tau = 10\,ns$, $B = 7\,T$, $T_{1,qubit} = 17\,\mu s$, $T_{2,qubit} = 680\,ns$, $T_{2,switch} = 2.3\,\mu s$)	NMR ($\tau = 25\,\mu s$, $T_{1,min} = 3.0\,\mu s$, $T_{2,min} = 1.2\,\mu s$)
fredkin110	86.73% (+10.27%)	98.59% (+0.79%)
halfadder	87.66% (+9.80%)	98.66% (+0.73%)
grover010	49.19% (+26.31%)	91.00% (+5.73%)
qft3	76.53% (+22.27%)	97.33% (+3.77%)
teleport [9]	88.92% (+10.07%)	98.75% (+0.47%)
qpeminus	84.18% (+15.58%)	98.73% (+2.50%)

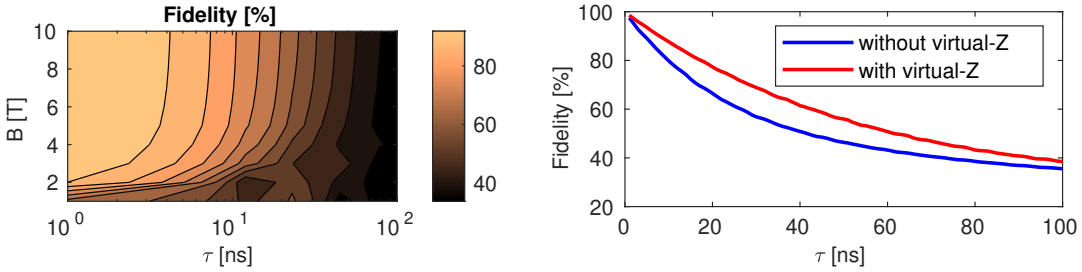

(a) Dependency of the fidelity on pulse duration and magnetostatic field, without virtual-Z gates.

(b) Comparison of fidelities provided by the quantum circuits with and without virtual-Z strategy, for $B = 7\,T$.

Fig. 5. Fidelity of reversible Half-adder in Cr_7Ni molecular nanomagnets.

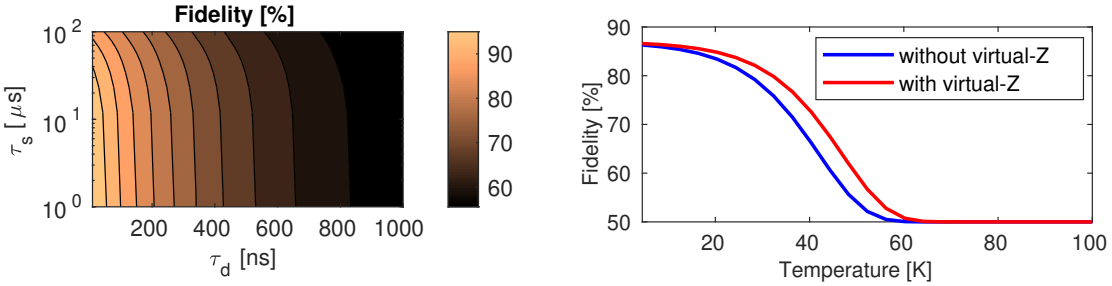

(a) Dependency of the fidelity on pulse durations of single and two-qubit gates, without virtual-Z gates, for $T = 4.5\,K$.

(b) Dependency of fidelity on temperature, for $\tau_s = 10\,\mu s$ and $\tau_d = 150\,ns$.

Fig. 6. Fidelity of Grover's search in vanadyl architecture.

REFERENCES

[1] M. A. Nielsen and I. L. Chuang, *Quantum Computation and Quantum Information: 10th Anniversary Edition*, 10th ed. New York, NY, USA: Cambridge University Press, 2011.

[2] T. Xin, B.-X. Wang, K.-R. Li, X.-Y. Kong, S.-J. Wei, T. Wang, D. Ruan, and G.-L. Long, "Nuclear magnetic resonance for quantum computing: Techniques and recent achievements," *Chinese Physics B*, vol. 27, no. 2, p. 020308, feb 2018.

[3] L. M. Vandersypen, M. Steffen, G. Breyta, C. S. Yannoni, M. H. Sherwood, and I. L. Chuang, "Experimental realization of shor's quantum factoring algorithm using nuclear magnetic resonance," *Nature*, vol. 414, no. 6866, p. 883, 2001.

[4] X. Kong, S. Wei, J. Wen, T. Xin, and G.-L. Long, "Experimental simulation of shift operators in a quantum processor," *Phys. Rev. A*, vol. 99, p. 042328, Apr 2019.

[5] A. Singh, H. Singh, K. Dorai, and Arvind, "Experimental classification of entanglement in arbitrary three-qubit pure states on an nmr quantum information processor," *Phys. Rev. A*, vol. 98, p. 032301, Sep 2018.

[6] J. Ferrando-Soria, E. Moreno Pineda, A. Chiesa, A. Fernandez, S. A. Magee, S. Carretta, P. Santini, I. J. Vitorica-Yrezabal, F. Tuna, G. A. Timco, E. J. L. McInnes, and R. E. P. Winpenny, "A modular design of molecular qubits to implement universal quantum gates," *Nature Communications*, vol. 7, no. 1, p. 11377, 2016.

[7] A. Chiesa, P. Santini, and S. Carretta, "Supramolecular complexes for quantum simulation," *Magnetochemistry*, vol. 2, no. 4, p. 37, 2016.

[8] M. Atzori, A. Chiesa, E. Morra, M. Chiesa, L. Sorace, S. Carretta, and R. Sessoli, "A two-qubit molecular architecture for electron-mediated nuclear quantum simulation," *Chem. Sci.*, vol. 9, pp. 6183–6192, 2018.

[9] G. A. Cirillo, G. Turvani, and M. Graziano, "A quantum computation model for molecular nanomagnets," *IEEE Transactions on Nanotechnology*, vol. 18, pp. 1027–1039, 2019.

[10] A. W. Cross, L. S. Bishop, J. A. Smolin, and J. M. Gambetta, "Open quantum assembly language," 2017.

[11] D. C. McKay, C. J. Wood, S. Sheldon, J. M. Chow, and J. M. Gambetta, "Efficient z gates for quantum computing," *Phys. Rev. A*, vol. 96, p. 022330, Aug 2017.

[12] A. Zulehner and R. Wille, "Advanced simulation of quantum computations," *Trans. on CAD of Integrated Circuits and Systems*, vol. 38, no. 5, pp. 848–859, 2019.